# Global scaling properties of a chaotic attractor reconstructed from experimental data

H. Atmanspacher, H. Scheingraber, and W. Voges
*Max-Planck-Institut für Physik und Astrophysik, Institut für Extraterrestrische Physik, D-8046 Garching, Federal Republic of Germany*

(Received 18 May 1987; revised manuscript received 21 August 1987)

Several aspects of attractor reconstruction and analysis using the method of correlation integrals have been thoroughly investigated for a specific chaotic attractor. Requirements on the experimental data, the generation of the artificial phase space, and the evaluation of the correlation integral are considered in detail. In order to explain the surprisingly smooth behavior of the correlation integrals resulting in an unusually straightforward and accurate analysis, the global scaling properties of the attractor are derived. They indicate that specific aspects of the analysis are a direct consequence of the structure of the attractor. Moreover, the scaling properties provide a useful criterion for an optimum adaption of the length of the required time series to the particular attractor under consideration.

## I. INTRODUCTION

It is presently well known that chaotic (strange) attractors represent a very universal behavior of dissipative nonlinear dynamical systems,[1] leading to remarkable aspects for fundamental physical concepts.[2] A chaotic attractor can be quantitatively characterized either by its metric properties (giving rise to static, time-independent invariants) or by dynamical invariants describing details of the temporal evolution of the considered system.[3]

The most commonly used invariants in the latter context are the Lyapunov exponents and the dynamical entropy (Kolmogorov entropy) of the system. The metric structure of the attractor, which will mainly be referred to in this work, can be characterized by the dimension of the attractor. More exactly, one can define a continuous spectrum of dimensions by means of a generalized information theoretical treatment.[4,3] We shall discuss these concepts briefly in Sec. II.

The attractor of a dynamical system can easily be obtained if the (nonlinearly) coupled differential equations for the relevant variables of the system are known. However, in many experimental situations neither the relevant variables nor even their total number are known, so that the attractor of the system is not *a priori* accessible. In this case, the attractor can be reconstructed in an artificial phase space, if a time series of one single variable is measured.[5,6] The embedding theorem of Takens[6] ensures that the attractor is reliably reconstructed in the limit of a sufficiently large dimension $d$ ($d \rightarrow \infty$) of the artificial phase space.

Based on this theorem, different procedures have been developed in order to determine dynamical as well as static invariants of attractors from experimental time series of single variables. In particular, we mention (1) the "nearest-neighbor method,"[7,8] (2) the "correlation integral method,"[9,10] and (3) the "singular system method."[11]

Some information about the quality of the results obtained with the different methods has been reported recently.[12] Although there is only limited experience with method (3) to date, this method is supposed to be particularly advantageous in case of rather noisy signals. Methods (1) and (2) can be considered equally reliable in case of low dimensions. For high-dimensional attractors, the nearest-neighbor procedure probably provides more exact results.[13]

In the present paper we investigate a low-dimensional attractor by means of method (2). The theoretical basis of this method is summarized in the context of Sec. II, which also contains the extension of the correlation integral concept towards the evaluation of generalized dimensions.[14] Their relationship to global scaling properties of the entire attractor[15] will be described.

Section III gives some details of the investigated system and the experimental time series, respectively. This time series represents the x-ray luminosity of the neutron star Her X-1, observed by the European x-ray satellite EXOSAT. An extended discussion of the attractor analysis with respect to its astrophysical relevance is published elsewhere.[16,17] In principle, the investigated processes show some rough analogy to hydrodynamical turbulence.

The original motivation for studying the astrophysical system Her X-1 was to gain information about the complexity of the radiation transport processes in the neutron star atmosphere. As it turned out, the analyzed x-ray data give rise to an attractor with the following interesting properties:[16] (i) the correlation integral yields extraordinarily smooth curves with only 1000 data points per time series; (ii) the spectrum of dimensions of positive order $q$ turns out to be almost independent of $q$. Because of these remarkable features, a detailed description and discussion of the attractor properties appeared to be interesting from the viewpoint of dynamical systems theory.

In Sec. IV we address some issues and problems which often arise in the correlation integral method. The following main points will be discussed: (i) requirements on the experimental time series (length, resolution); (ii) generation of the artificial phase space (phase-space portraits, appropriate time delay); (iii) evaluation of the correlation integral (linear scaling region; convergence of slopes). These aspects will be exemplified by the corresponding features observed in the analysis of the Her X-1 data.

In Sec. V the spectra of dimensions and of singularities are determined, which characterize the global scaling properties of the attractor. These properties can to some extent explain the unusually smooth correlation integrals and the corresponding accuracy in determining the attractor dimensions. More importantly, the global scaling properties are shown to provide quantitative criteria for a sufficient reconstruction of an attractor, particularly for a sufficient length of the required time series. The main results are summarized in Sec. VI.

## II. SCALING PROPERTIES OF CHAOTIC ATTRACTORS

As previously indicated, we restrict ourselves to a characterization of attractors in terms of their metric properties. This means that we consider an extended complex object in phase space without explicit respect to its temporal evolution. This object, the chaotic attractor, represents that subspace of the entire phase space on which the trajectory of the considered system is asymptotically situated. In principle, the metric properties of the attractor are therefore of nondynamical character. However, it has been shown that there are strong relationships between metric and dynamical invariants.[18,19]

### A. Generalized dimensions

A suitable quantity characterizing the attractor as a metric structure is its dimension. For chaotic attractors, this usually takes on noninteger values, thus generalizing the traditional imagination of purely integer dimensions. The latter case denotes regular (stationary, periodic) processes. The concept of a fractal (noninteger) dimension $D<d$ of an attractor in a $d$-dimensional phase space can be derived from information theoretical considerations, where the dimension $D$ describes how the information $I_\epsilon$ scales with varying spatial resolution $\epsilon$ according to

$$D=\lim_{\epsilon\to 0}\frac{I_\epsilon}{\log_2(1/\epsilon)} \ . \tag{1}$$

For a formal introduction of the information $I_\epsilon$ as we shall use it, we consider a partition of the attractor into $m$ boxes of size $\epsilon$. The probability that a point on the trajectory falls into the $i$th box is then given by $p_i=N_i/N$ if $N$ is the total number of points. Using this probability, a generalized information of order $q$ ($q\in R$) is defined as[20]

$$I^{(q)}=\frac{1}{1-q}\log_2\left[\sum_{i=1}^{m}p_i^q\right] , \tag{2}$$

which reduces to the well-known Shannon information[21] for $q\to 1$.

On the basis of $I^{(q)}$, a continuous spectrum of dimensions of order $q$ is introduced[4] by substituting $I^{(q)}$ into Eq. (1),

$$D^{(q)}=\frac{1}{q-1}\lim_{\epsilon\to 0}\frac{\log_2\left[\sum_{i=1}^{m}p_i^q\right]}{\log_2\epsilon} \ . \tag{3}$$

The most frequently used dimensions $D^{(q)}$ are the Hausdorff (or fractal) dimension $D^{(0)}$, the information dimension $D^{(1)}$, and the correlation dimension $D^{(2)}$. For the total set of generalized dimensions it can be shown that

$$D^{(q)}\le D^{(q')} \quad \text{if } q'\le q \tag{4}$$

where the equality holds for a completely homogeneous probability distribution $p_i=1/N$. Hence, the difference between dimensions of different order measures the degree of inhomogeneity (or nonuniformity) of the attractor in the sense of whether its different subsets (boxes) are visited with equal frequency.

For the reconstruction of an attractor from a single-variable time series, the method proposed by Grassberger and Procaccia[9] uses the dimension $D^{(2)}$, which is derived from the correlation integral,

$$C_\epsilon^{(2)}=\lim_{\epsilon\to 0}\frac{1}{N^2}\sum_{i,j=1}^{N}\Theta(\epsilon-|\mathbf{x}_i-\mathbf{x}_j|) \ . \tag{5}$$

Here $N$ is the number of data points recorded with the temporal resolution $\tau$. The points $\mathbf{x}_i$ have been constructed by a time delay ($\Delta t$) technique[6] generating the artificial phase space which is used to reconstruct the attractor of the actual process. The Heaviside function $\Theta(\epsilon-|\mathbf{x}_i-\mathbf{x}_j|)$ serves to count how many pairs of points $(\mathbf{x}_i,\mathbf{x}_j)$ fall within the distance $\epsilon$.

Recently the procedure of Grassberger and Procaccia has been extended to a calculation of dimensions of arbitrary order $q$ by a corresponding correlation integral $C_\epsilon^{(q)}$,[14]

$$C_\epsilon^{(q)}=\lim_{\epsilon\to 0}\left[\frac{1}{N}\sum_{i=1}^{N}\left[\frac{1}{N}\sum_{j=1}^{N}\Theta(\epsilon-|\mathbf{x}_i-\mathbf{x}_j|)\right]^{q-1}\right]^{1/q-1} . \tag{6}$$

Using this correlation integral, the dimension of order $q$ is given by

$$D^{(q)}=\lim_{\epsilon\to 0}\frac{\log_2 C_\epsilon^{(q)}}{\log_2\epsilon} \ . \tag{7}$$

For the case $q=2$, the exponents of both summations in Eq. (6) are equal to one. This situation considerably facilitates the numerical work. For $q\neq 2$ the calculation is more involved since each individual sum has to be raised to the corresponding power. However, the increase in numerical effort is tolerable, particularly compared with the computing time required for direct box counting algorithms.[14]

The spectrum of dimensions $D^{(q)}$ using Eq. (7) contains more detailed information about the metric properties of the attractor than each single dimension does. This is understandable as at different order $q$ different subsets on the attractor become dominant in the determination of $C^{(q)}$ and $D^{(q)}$. Intuitively, the variation of $q$ provides a scan through all degrees of point density existing along the trajectory.

### B. Spectrum of singularities

The concept of generalized dimensions reviewed in Sec. II A can be related to the work of Halsey *et al.*[15] in which the global scaling properties of the attractor are considered in detail. The unifying element between both formalisms is given by the probability $p_i$ defined previously. For the present this probability is

$$p_i(\epsilon)=\epsilon^{\alpha_i(\epsilon)} , \tag{8}$$

where $\alpha_i(\epsilon)$ is a scaling index describing how the variation of probability versus the variation of $\epsilon$ departs from linearity. For decreasing $\epsilon$, the probability decreases much faster for large than for small $\alpha$. Therefore, the scaling index $\alpha$ provides a measure for the density of points on different subsets of the attractor. Large values of $\alpha$ characterize the rarefied subsets, whereas small values of $\alpha$ represent the dense subsets. Typically, a limited range $\alpha_{\min}<\alpha<\alpha_{\max}$ is obtained for a particular attractor (see the examples in Refs. 14 and 15). The quantity $\alpha_{\min}-\alpha_{\max}$ roughly measures the degree of nonuniformity (or inhomogeneity) of the attractor.

The point density spectrum on the attractor is equivalent to a spectrum of singularities in the probabilities $p_i$. (In this more technical language, the scaling index $\alpha$ represents the strength of the singularity.) In order to find the "intensities" of the spectral components $\alpha$, one has to compute how often singularities of strength $\alpha$ occur. The singularity density $\rho(\alpha)$ defines the number of times $n_\epsilon(\alpha)$ that a singularity of strength $\alpha\in[\alpha',\alpha'+d\alpha']$ occurs on the attractor partitioned with resolution $\epsilon$,

$$n_\epsilon(\alpha)=d\alpha'\rho(\alpha')\epsilon^{-f(\alpha')} . \tag{9}$$

Here, the continuous function $f(\alpha)$ is an index which reflects the scaling of $n_\epsilon(\alpha)$ as a function of $\epsilon$.

Connecting Eqs. (8) and (9) with Eq. (3), Halsey *et al.* derived a formal relationship between the spectrum of dimensions $D^{(q)}$ and the spectrum of singularities $f(\alpha)$. It consists of a Legendre transformation given by

$$\alpha(q)=\frac{d}{dq}[(q-1)D^{(q)}] \tag{10}$$

and

$$f[\alpha(q)]=q\alpha(q)-(q-1)D^{(q)} . \tag{11}$$

Equations (10) and (11) enable an easy calculation of $f(\alpha)$ for a spectrum of $D^{(q)}$ which can be obtained using the correlation integral $C^{(q)}$.

The function $f(\alpha)$ shows the following universal properties:

$$\frac{df}{d\alpha}=q , \tag{12}$$

$$\frac{d^2f}{d\alpha^2}<0 , \tag{13}$$

from which it follows that

$$D^{(0)}=f_{\max}(\alpha) , \tag{14}$$

$$D^{(-\infty)}=\alpha_{\max} , \tag{15}$$

$$D^{(\infty)}=\alpha_{\min} . \tag{16}$$

In the following we shall see how all these features appear in the investigated attractor. Moreover, the degree of nonuniformity will be applied as a criterion for the choice of experimental and numerical parameters used to reconstruct the attractor.

## III. INVESTIGATED SYSTEM: THE ACCRETING NEUTRON STAR HER X-1

Together with its visible companion HZ Her, the neutron star Her X-1 forms a rotating binary system. Due to its strong gravitational potential, Her X-1 accretes gaseous matter from HZ Her. This matter surrounds Her X-1 in an "accretion disk" from which matter streams down onto the neutron star surface. In case of Her X-1, a strong magnetic field channels the accreting matter on to the polar regions. The deceleration of the infalling matter in the vicinity of the star surface produces a significant x-ray emission discovered by the satellite UHURU in 1971.[22]

Due to the complex geometry of the entire binary system (two stars rotate around a common center of mass; one of them is surrounded by a warping accretion disk) distinct time periods coexist. They are attributable solely to geometrical and shadowing effects. In addition to these effects, we have recently[16] shown evidence for low-dimensional chaos with a remarkable stochastic component determining the process of the x-ray radiation transport through the neutron star atmosphere (source mode *A* in Ref. 16). This evidence has been obtained by determining attractor dimensions from different x-ray luminosity time series in different geometrical configurations of the binary system according to the procedure of Grassberger and Procaccia.[9]

The time series used in the analysis have been obtained by the x-ray satellite EXOSAT. The data contain integral counts of the source (including background) in the energy range 1–50 keV and were recorded with a temporal resolution of 9.67 msec.

Further astrophysical details are given elsewhere.[16] In Sec. IV attention is directed to some extraordinary features occurring in the attractor reconstruction and analysis.

## IV. SPECIFIC ASPECTS OF THE ATTRACTOR ANALYSIS

The Her X-1 data investigated here provided an exceptionally "well-behaved" attractor analysis using the correlation integral method. Even with 1000 data points per time series, the reconstruction of the attractor worked out perfectly. The correlation integral curves ($\log_2 C_\epsilon^{(2)}$ versus $\log_2\epsilon$) showed a smoothness unusual for experimental time series data as short as mentioned. An example is shown in Fig. 1 of Ref. 16. This behavior suggests a further investigation with particular respect to its system theoretical issues. The present section is consequently organized following the successive steps of the correlation integral procedure.

### A. Requirements upon experimental data

The main points under this title concern the length and the temporal resolution of the measured time series. To start with the latter one, the resolution $\tau$ has been proposed[23] to be chosen in a way that some ten data points fall into a correlation period of the investigated process. This correlation period $t_{\mathrm{corr}}$ itself can be determined by an autocorrelation analysis. Too few data points per correlation period incorrectly yield an uncorrelated (stochastic) process.

There is no basic upper limit to the number of data points per correlation period. However, a practical limit exists if the signal amplitude becomes very small due to high temporal resolution $\tau$. Then the (stochastic) influence of counting statistics prevents an identification of possibly underlying deterministic chaos.

The process investigated exhibits correlation periods of $10\pm3$ sec.[16] A proper temporal resolution $\tau$ should therefore be given by some 100 msec. Indeed, a corresponding value of $\tau$ has impressively confirmed the above arguments. Too low and too high values of $\tau$ did not lead to a convergent behavior of the slope of the correlation integral curves with increasing embedding dimension (see also Sec. IV C). Excellent convergence has been obtained for $\tau\approx770$ msec [see time series (6d) in Table II of Ref. 16]. This resolution was simply produced by integrating the original 9.67-msec resolution data.

The length of the time series, i.e., the total number $N$ of data points, represents a second significant problem for the attractor analysis. Without any respect to possible experimental constraints on $N$, time series of 500 to 1000 data points have been shown[24] to be sufficient for a reasonable estimate of the attractor dimension $D^{(2)}$. However, the accuracy of the determination of this dimension is generally not very high if $N$ is substantially smaller than $10^4$.

Nevertheless, we emphasize that the smoothness of $C_\epsilon^{(2)}$ (as an important precondition for an accurate determination of $D^{(2)}$) often depends critically on the number $N$ of data points per time series. In addition, $N$ limits the reasonable embedding dimension $d$ of the artificial phase space. With increasing dimension, the number of pairs of points with small distances decreases, thus leading to statistically poor results for too high dimensions.

The question of a sufficient number $N$ of data points is important since the required computing time varies quadratically with $N$. Moreover, experimental circumstances may arise which restrict a measurement of time series to less than an optimum number of correlation periods. (Here we meet the requirements on $\tau$.) Thus, it is desirable to have a reliable criterion for a sufficient value of $N$. In Sec. V we derive such a criterion and demonstrate its operation.

### B. Generation of the artificial phase space

The experimental time series is used to generate the artificial phase space in which the attractor is to be reconstructed. As shown in Sec. II, the delay technique shifts the time series by a time delay $\Delta t = l\tau$, where $l$ has to be chosen so that the desired sequence of time series is linearly independent.

A clever idea to determine an optimum value of $\Delta t$ is based on the concept of mutual information.[25] Its application is, however, problematic, if only a low number of data points per time series is available. The reason is the following: Each particular shift causes a number of $l=\Delta t/\tau$ data points out of the measured time series to

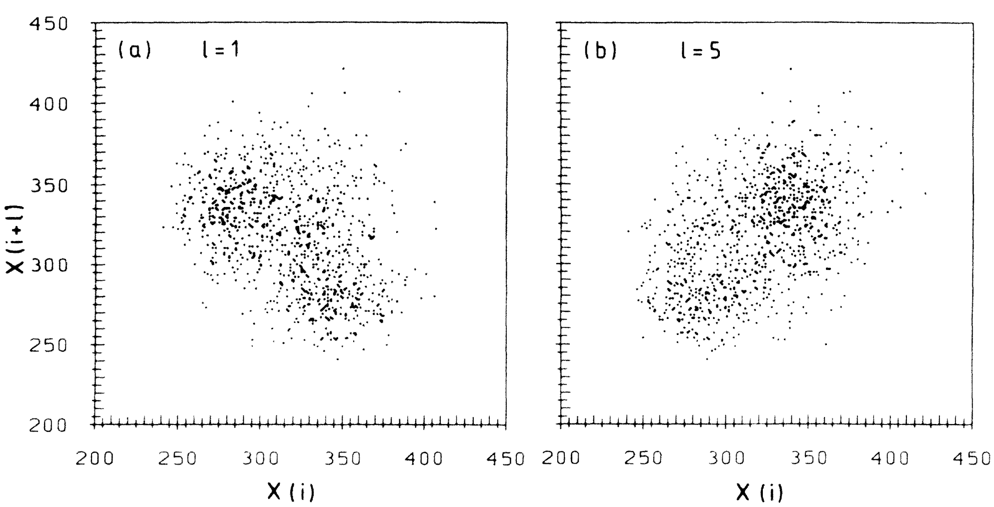


FIG. 1. Phase-space portraits of the investigated time series containing $N=1000$ data points. $X(i)$ is plotted vs $X(i+l)$. The time delay used to generate the artificial phase space is given by $\Delta t = l\tau$, where $\tau$ is the temporal resolution of the time series. (a) and (b) show the situation for $l=1$ and $l=5$, respectively. Both situations provide a distribution of points which clearly deviates from $X(i)=X(i+l)$. This case would indicate a linear dependence of the shifted data sets.

become unutilizable for the analysis. Since the optimum $\Delta t$ according to the mutual information concept is usually considerably larger than the correlation period $t_{\rm corr}$,[25] there may be up to some hundred data points per time series which remain unused. For a $d$-dimensional phase space, this means that possibly some hundred data points more than finally required have to be measured.

As this procedure is not practicable for short time series, we use the approximate test of a suitable $\Delta t$ by means of two-dimensional representations of the time series $X(i)$ versus $X(i+l)$, giving a phase-space portrait of the attractor. In Fig. 1 we show such a phase-space portrait for $l=1$ [Fig. 1(a)] and $l=5$ [Fig. 1(b)]. The plotted points represent a series of 1000 data points recorded with a resolution of 770 msec. Neither in Figs. 1(a) and 1(b) nor for $l=2,3,4$ is there a tendency of accumulation around the line $X(i)=X(i+l)$. Hence, there is no significant linear dependence between both time series. Moreover, the similarity of Figs. 1(a) and 1(b) shows that the analysis is not very critical with respect to $\Delta t$. (This is also noted in the determination of $C_\epsilon^{(2)}$ for different values of $\Delta t$.)

We now inquire into changes in the phase-space portraits with decreasing number $N$ of data points. The corresponding plots can then provide a qualitative idea of whether the representation with few points is a good or bad approximation for a representation using more points. Figure 2 visualizes the phase-space portrait ($l=1$) for only 200 successive points out of the time series shown in Fig. 1. The qualitative impression of the distribution does not much differ from that in Fig. 1. Moreover, it is even not remarkably different for different sets of selected points [Fig. 2(a): 201–400; Fig. 2(b): 401–600]. In spite of the subjective nature of this argument, it provides some indication for low requirements on a sufficient length of the time series. We shall quantitatively confirm this argument at a later stage.

### C. Evaluation of the correlation integral

Using Eq. (5), the correlation integral $C_\epsilon^{(2)}$ is calculated for successive embedding dimensions $d$. Two salient points are [cf. Eq. (7)]: (i) the determination of the linear scaling range of $\log_2 C_\epsilon^{(2)}$ versus $\log_2\epsilon$, required to derive the slope $\nu$; (ii) the convergence behavior of $\nu$ for increasing $d$.

A linear scaling range can be demonstrated by a plot of the slope $\nu$ between successive calculated values of $\log_2 C_\epsilon^{(2)}$ versus $\log_2\epsilon$. The embedding dimension $d$ is an additional parameter in such a plot. Figure 3 shows $\nu$ as a function of $\log_2\epsilon$ for $1<d<40$. The analyzed time series is the same as used for Fig. 1. The smoothness of the plots reflects the smoothness of the correlation integral curves.

A pronounced plateau exists at $2<\nu<3$. For sufficiently high embedding dimension ($d>8$) it extends over $\Delta\log_2\epsilon\approx 0.5$. The plateau corresponds to a constant slope of $\log_2 C_\epsilon^{(2)}$ versus $\log_2\epsilon$, and thus represents a linear scaling range. The increasing slope toward lower values of $\epsilon$ means that only at high signal amplitudes (corresponding to high values of $\epsilon$) does a low-dimensional attractor appear. For small amplitudes, the behavior of the measured luminosity indicates stochasticity, probably noise. Such a feature has already been observed in the analysis of numerically simulated as well as experimental data.[26,27] The extension of the linear range toward low $\epsilon$ is limited by stochastic contributions. For example, $d=20$ provides $\epsilon<2^{7.5}$ for the noise dominated regime and $\epsilon=2^{8.5}$ for the characteristic size of the attractor, i.e., a noise level of 50%. For a further integration of the raw data, yielding a better statistics, we obtain no linear range since $\tau$ becomes too large to show correlated behavior.

In Fig. 3 it seems that the slope is slowly increasing with embedding dimension $d$. This impression is due to

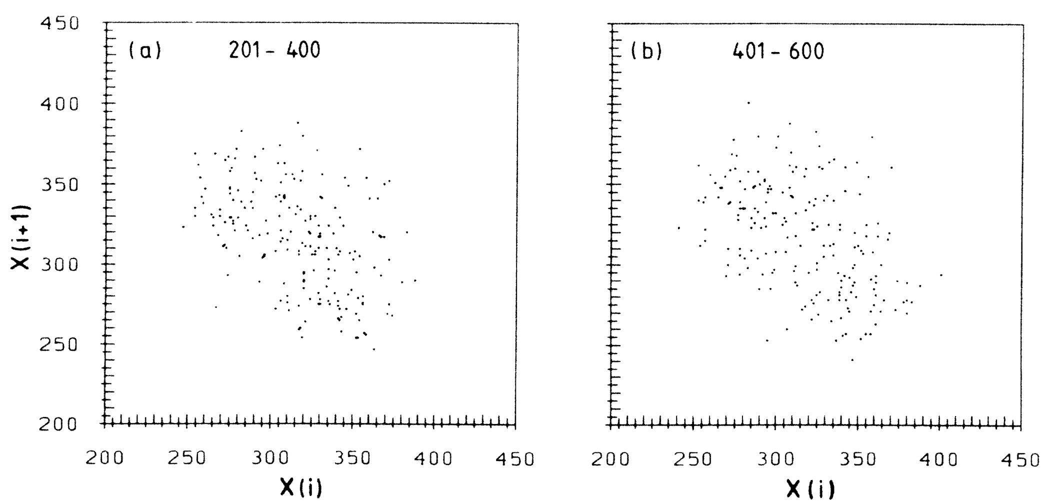


FIG. 2. Phase-space portraits of two different temporal sections of the time series used in Fig. 1. These sections contain $N=200$ points and are both plotted for $l=1$. Points 201–400 and 401–600 are shown in (a) and (b), respectively. They indicate a sufficient covering of the attractor with a very low number of data points.

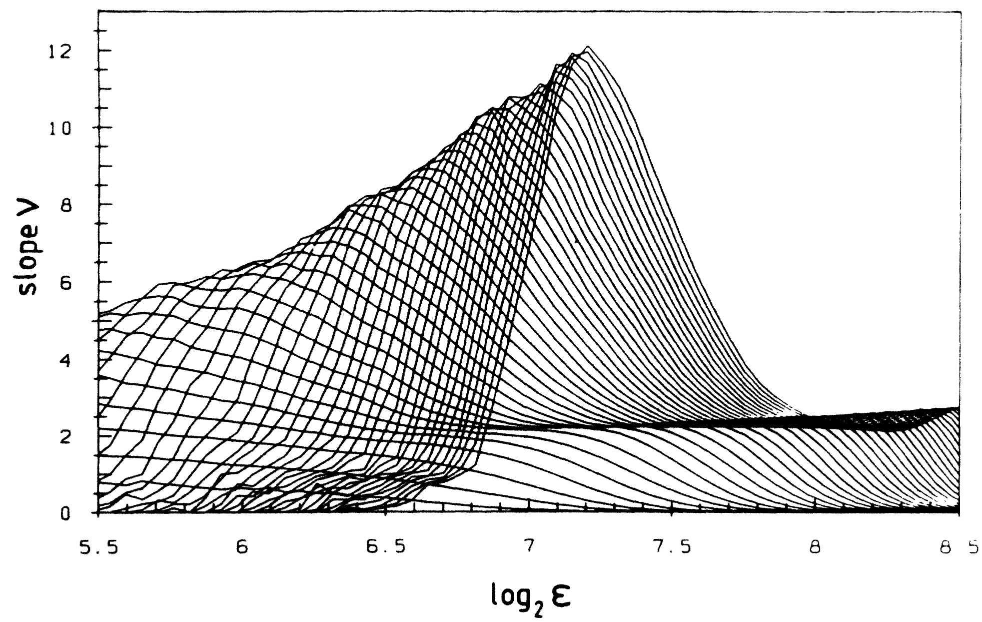


FIG. 3. Slope $\nu$ of the logarithm of the correlation integral ($\log_2 C_\epsilon^{(2)}$) vs $\log_2\epsilon$ up to $d=40$. The distinct plateau with $\nu\approx 2.3$ indicates the linear scaling range for each particular $d$ as well as the convergence of $\nu$ for increasing $d$. This situation describes low-dimensional chaos ($D^{(2)}\approx 2.3$).

the fact that there appears an increasingly pronounced hump where the linear range is left toward larger $\epsilon$. A possible reason for this is boundary effects of the attractor;[27] when $\epsilon$ approaches the size of the attractor, its boundary contributes a larger amount of data to $C_\epsilon$, thus locally increasing the slope. The influence of this effect grows with $d$, since the relative number of data points constituting the boundary increases.

## V. GLOBAL SCALING PROPERTIES OF THE HER X-1 ATTRACTOR

In Sec. IV the main issues brought out were (i) qualitatively identical phase-space portraits with different subsets of points; (ii) exceptional smooth curves of $\log_2 C_\epsilon^{(2)}$ versus $\log_2\epsilon$ as well as for $\nu$ versus $\log_2\epsilon$.

We now explore the origin of these remarkable results. To this end, we use the extended concept of dimension $D^{(q)}$ of arbitrary order $q$ and the spectrum of singularities $f(\alpha)$ as introduced in Sec. II. As in Sec. IV, we consider only the attractor representing time series (6d) in Table II of Ref. 16.

### A. Spectrum of dimensions

The determination of $D^{(q)}$ is carried out according to Eqs. (6) and (7) of Sec. II. For the present purposes, the correlation integral $C_\epsilon^{(q)}$ is determined for $d=20$ which ensures a complete embedding of an attractor with $D^{(2)}<3$. The sufficiency of $d=20$ will become evident if the spectrum $D^{(q)}$ does not provide dimensions considerably larger than $D^{(2)}$.

The calculated correlation integrals $C_\epsilon^{(q)}$ $(-22<q<22)$ for $d=20$ are given in Fig. 4(a). For reasons to be discussed below, time series of 2000 data points have been used. As it was the case for $C_\epsilon^{(2)}$, the smoothness of the curves is impressive. In order to obtain $D^{(q)}$ from $C_\epsilon^{(q)}$, we proceeded as described in Secs. IV B and IV C.

The resulting spectrum of dimensions $D^{(q)}$ for a stepwidth $\Delta q=0.25$ is shown in Fig. 4(b). The errors have been obtained as the standard errors of a least-squares fit over the linear scaling range of $C_\epsilon^{(q)}$ for each particular value of $q$. The general form of $D^{(q)}$ as a function of $q$ is in agreement with the condition given by Eq. (4): $D^{(q)}$ decreases with increasing $q$. For high values of $|q|$, $D^{(q)}$ converges towards $D^{(+)}\approx 2.2$ and $D^{(-)}\approx 3.5$. The low latter value confirms that a dimension $d=20$ still provides complete embedding.

A striking detail of the $D^{(q)}$ spectrum is the almost constant dimension for $q>0$. Of course, $D^{(2)}=2.30$ agrees with the formerly determined value.[16] The value of $D^{(0)}=2.37$ is still not much larger than $D^{(2)}$. A considerable increase of $D^{(q)}$ only appears at negative $q$. The errors are smallest for small $|q|$.

$C_\epsilon^{(q)}$ and $D^{(q)}$ in Figs. 4(a) and 4(b) have been calculated from a time series containing 2000 data points. This deviation from $N=1000$ is motivated by the idea of comparing the $D^{(q)}$ spectrum for time series of different length. If a time series were too short to reflect the entire scaling properties of an attractor reliably, it is expected that the point densities within the attractor are more inhomogeneously distributed than for a sufficient number of data points. This fact has been clearly demonstrated for numerically simulated time series.[14] Figure 2(a) in Ref. 14 shows a significant increase of $\alpha_{\max}-\alpha_{\min}=D^{(-\infty)}-D^{(\infty)}$ [cf. Eqs. (15) and (16)] in the $f(\alpha)$ spectrum if the length is lowered from 4000 to

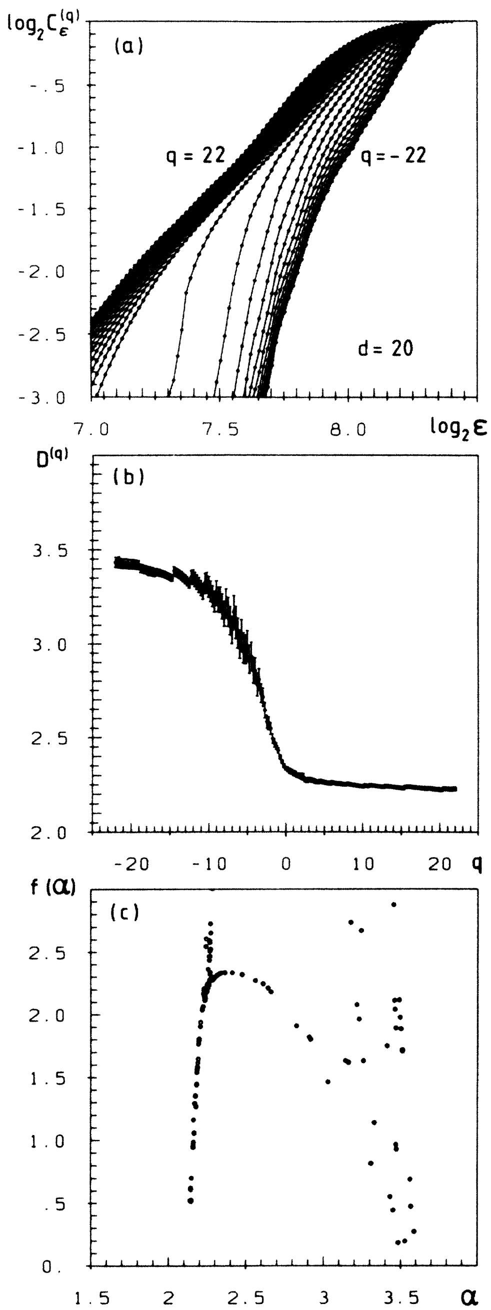


FIG. 4. Derivation of the global scaling properties of a low-dimensional chaotic attractor reconstructed from 2000 data points in a phase space of dimension $d=20$ according to the correlation integral method (Ref. 14). (a) Logarithm of the correlation integral $C_\epsilon^{(q)}$ vs $\log_2 \epsilon$, obtained from Eq. (6). The different curves show the range $-22<q<22$ in steps of $\Delta q=2$. (b) Generalized dimensions $D^{(q)}$ [Eq. (7)] as derived from the relevant linear scaling range. The errors represent the standard errors of the least-squares fit yielding the slope $\nu$ for each particular $q$ (stepwidth $\Delta q=0.25$). The errors grow with decreasing $q$. (c) The $f(\alpha)$ spectrum due to Eqs. (10) and (11), as obtained from the dimensions in (b). Although the typical shape of an $f(\alpha)$ curve can already be recognized, there are a lot of irregularly distributed points. Note particularly the steep branch marginally appearing at $\alpha \approx 3.6$.

2000 points. The difference $D^{(-\infty)}-D^{(\infty)}$ just provides the required measure of inhomogeneity. This difference should converge if the attractor is covered by a sufficient number of points reflecting its inherent scaling behavior.

In order to test this for the Her X-1 attractor we used the spectrum $D^{(q)}$ for additional time series of 560 and 1000 points. The differences $D_{560}^{(q)}-D_{2000}^{(q)}$ and $D_{1000}^{(q)}-D_{2000}^{(q)}$ for each particular $q$ then yield a spectrum of residua (Fig. 5) which clearly shows the equivalence of the spectra of dimensions. There are no additional inhomogeneities caused by the lower numbers of data points, compared with $N=2000$. (Note, however, that slight deviations occur in the range of negative $q$.) This quantitative result confirms the impression from Figs. 1 and 2. The correct structure of the attractor is available from relatively short time series. This information is valuable for the application of the correlation integral method since various steps of the method sensitively depend on the length of the time series (see Sec. IV).

### B. Spectrum of singularities

The spectrum of singularities $f(\alpha)$ can be obtained from $D^{(q)}$ using Eqs. (10) and (11). A direct application

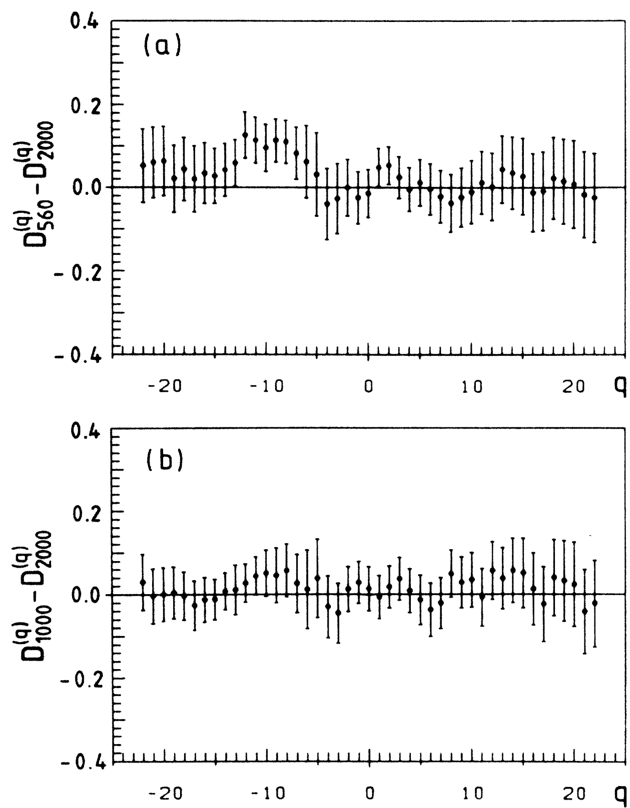


FIG. 5. Differences in the spectrum of $D^{(q)}$ for different numbers $N$ of data points per time series, shown using the residua $D_N^{(q)}-D_{N'}^{(q)}$. (a) $D_{560}^{(q)}-D_{2000}^{(q)}$; (b) $D_{1000}^{(q)}-D_{2000}^{(q)}$. Both figures give clear evidence for the fact that the spectrum of dimensions is almost identical (within its errors) for different $N$. Consequently, the investigated attractor is sufficiently reconstructed with time series of only 560 data points.

of these equations to the spectrum $D^{(q)}$ as shown in Fig. 4(b) yields Fig. 4(c). Within a couple of scattered points, the familiar form of an $f(\alpha)$ spectrum with the properties expressed by Eqs. (12)–(16) can be recognized.

Many of the scattered points result from the fact that the spectrum $D^{(q)}$ according to Fig. 4(b) partly provides positive derivatives $(d/dq)[(q-1)D^{(q)}]$ in Eqs. (10) and (11). Since such positive derivatives contradict Eq. (4), the spectrum $D^{(q)}$ must be smoothed before being transformed into $f(\alpha)$. We used a very simple smoothing procedure by performing a linear regression over $\Delta q=2$ for each $q$. The smoothed version of Fig. 4(b) is shown in Fig. 6(a).

The $f(\alpha)$ spectrum corresponding to the smoothed $D^{(q)}$ is presented in Fig. 6(b). The familiar shape shows

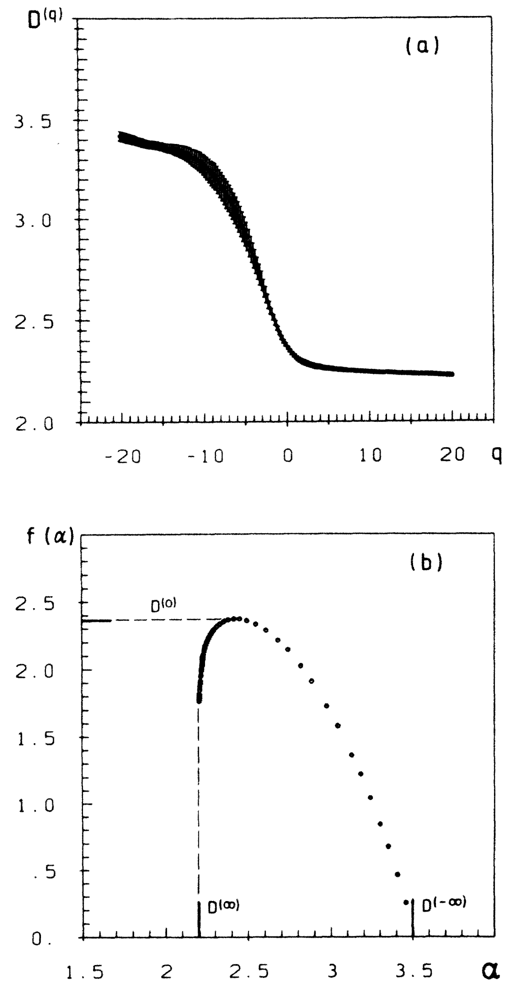


FIG. 6. (a) Spectra $D^{(q)}$ and (b) $f(\alpha)$ after smoothing the curve shown in Fig. 4(b). The applied smoothing procedure is described in the text. (b) represents $f(\alpha)$ as calculated for $q>-4.5$. $D^{(0)}$, $D^{(-\infty)}$, and $D^{(\infty)}$ are indicated according to Eqs. (14)–(16). The most characteristic features of $f(\alpha)$ are its strong asymmetry and the finite value of $f(\alpha_{\min})\approx 1.75$. All those points which are irregularly spread in Fig. 4(c) are now bound to the correct $f(\alpha)$ curve. However, we stress the peculiar behavior of $f(\alpha)$ corresponding to $q<-4.5$ which emphasizes the steep branch at $\alpha\approx 3.6$ in Fig. 4(c). See text for more details.

up much more clearly than in Fig. 4(c). The left branch (corresponding to positive $q$) does not reach $f(\alpha_{\min})=0$. This behavior, revealed only after smoothing of $D^{(q)}$, reflects the fact that the most concentrated subsets on the attractor do not represent ideal points (with dimension zero) but extended sets of points with dimension $f(\alpha_{\min})\approx 1.75$. The right branch provides still $f(\alpha_{\max})\approx 0$ for $\alpha_{\max}\approx 3.5$.

The regularly shaped $f(\alpha)$ spectrum in Fig. 6(b) only contains the $D^{(q)}$ spectrum for $q>-4.5$. All values of $D^{(q)}$ with $-12<q<-4.5$ transform into negative values of $f(\alpha)$ which cannot be seen in Fig. 6(b). The dimensions $D^{(q)}$ with $q<-12$ account for the peculiar steep branch arising at $\alpha\approx 3.6$ in Fig. 4(c). The negative values mentioned above represent an extension of this steep branch (see below).

The most remarkable features of the $f(\alpha)$ spectrum are the finite value of $f(\alpha_{\min})$ and its strong asymmetry. Both properties indicate that subsets with high point density on the attractor (corresponding to the left branch) are concentrated in a very narrow density range ($\alpha$ range). Higher values of $\alpha$ correspond to the more rarefied regions on the attractor. The frequency of their occurrence decreases continuously towards zero. Halsey *et al.* present similar situations in Figs. 5 and 12 of Ref. 15. They also report problems with the calculation of the flat branch of $f(\alpha)$ although performing a different kind of analysis. In addition, we mention that previous determinations of $f(\alpha)$ from experimental data for a Rayleigh-Bénard system[28,29] show increasing errors for increasing $\alpha$.

The particular form of the $f(\alpha)$ spectrum of the Her X-1 attractor suggests a possible reason for the repeatedly mentioned accurate results from the correlation integral analysis. The attractor is apparently dominated by its concentrated subsets of almost equal density ($\alpha_{\min}$). Hence, the dominant properties of the attractor can be extracted using a rather low number of points; most of them are situated in the dense subsets characterized by positive $q$.

This line of argument also gives a possible reason for the problematic determination of those $f(\alpha)$ corresponding to large negative orders $q$. For even with $N=2000$ the number of points might be too low for a sufficient representation of the scaling behavior in the rarefied regions of the attractor. Thus, the values of $f(\alpha)$ corresponding to $q<-4.5$ would indeed turn out to be caused by a paucity of data points in the rarefied regions of the attractor.

## VI. SUMMARY

The presented investigations pursue the following twofold intention.

(1) They describe a couple of methodical details complementary to our recent work on deterministic chaos in an astrophysical context.[16] These details might be valuable and helpful under the general viewpoint of the analysis of attractors.

(2) The attractor of the investigated system revealed specific properties leading to essential eases for its

analysis. Its global scaling behavior indicates reasons for the accuracy of the results obtained by the correlation integral method.[9,14]

The attractor analysis has been carried out for the process generating irregular variations of the x-ray radiation from the neutron star Her X-1. The global scaling properties of the attractor, i.e., the spectrum of dimensions and the spectrum of singularities, have been determined, respectively. The analysis provided extraordinarily smooth curves of the correlation integral for time series of only 1000 data points, thus enabling a clean and unproblematic determination of $D^{(q)}$. As a second surprising result, dimensions of positive order $q$ turned out to be almost independent of $q$.

A relation between these two features has been established using the spectrum of singularities of the attractor. It is roughly characterized by a strong asymmetry which stresses the dominance of subsets with high point density on the attractor. This asymmetry reflects the constancy of $D^{(q)}$ for $q>0$. Simultaneously it gives an idea of how to explain the low requirements on the necessary number of data points. These arguments show that the particular structure of the investigated attractor is responsible for the smoothness of the correlation integral curves and thus for the accuracy in determining $D^{(q)}$.

A valuable criterion for a sufficient length of the analyzed time series has been proposed. It makes use of the fact that too less data points cause inhomogeneities additional to those originating in the attractor itself. Since the degree of inhomogeneity can be quantified by the global scaling properties, a comparison of these properties for different numbers of data points allows for a determination of the minimum number needed for reliable results.

## ACKNOWLEDGMENTS

One of us (H.A.) gratefully acknowledges support by the Reimar Lüst Foundation. We thank H. G. Schuster for communicating the extension of the correlation integral method prior to publication. For a careful reading of the manuscript we are grateful to C. P. Sonett.

[1]J.-P. Eckmann and D. Ruelle, Rev. Mod. Phys. **57**, 617 (1985).
[2]H. Atmanspacher and H. Scheingraber, Found. Phys. **17**, 939 (1987), and further references therein.
[3]I. Procaccia, Phys. Scr. **T9**, 40 (1985).
[4]H. G. E. Hentschel and I. Procaccia, Physica (Utrecht) **8D**, 435 (1983).
[5]N. H. Packard, J. P. Crutchfield, J. D. Farmer, and R. S. Shaw, Phys. Rev. Lett. **45**, 712 (1980).
[6]F. Takens, in *Dynamical Systems and Turbulence,* Vol. 898 of *Lecture Notes in Mathematics,* edited by D. A. Rand and L. S. Young (Springer, Berlin, 1981).
[7]Y. Termonia and Z. Alexandrovitch, Phys. Rev. Lett. **45**, 1265 (1983).
[8]R. Badii and A. Politi, J. Stat. Phys. **40**, 725 (1985).
[9]P. Grassberger and I. Procaccia, Phys. Rev. Lett. **50**, 346 (1983).
[10]P. Grassberger and I. Procaccia, Phys. Rev. A **28**, 2591 (1983).
[11]D. S. Broomhead and G. P. King, Physica (Utrecht) **20D**, 217 (1986).
[12]J. Holzfuss and G. Mayer-Kress, in *Dimensions and Entropies in Dynamical Systems,* edited by G. Mayer-Kress (Springer, Berlin, 1986).
[13]R. Stoop (private communication).
[14]K. Pawelzik and H. G. Schuster, Phys. Rev. A **35**, 481 (1987).
[15]T. C. Halsey, M. H. Jensen, L. P. Kadanoff, I. Procaccia, and B. I. Shraiman, Phys. Rev. A **33**, 1141 (1986).
[16]W. Voges, H. Atmanspacher, and H. Scheingraber, Astrophys. J. **320**, 794 (1987).
[17]G. E. Morfill, V. Demmel, and H. Atmanspacher, Mitt. Astron. Ges. **68**, 251 (1987).
[18]P. Frederickson, J. L. Kaplan, E. D. Yorke, and J. A. Yorke, J. Differential Equations **49**, 185 (1983).
[19]M. J. Feigenbaum, M. H. Jensen, and I. Procaccia, Phys. Rev. Lett. **57**, 1503 (1986).
[20]J. Balatoni and A. Renyi, in *Selected Papers of A. Renyi,* edited by P. Turán (Akademiai K., Budapest, 1976), Vol. 1, p. 588.
[21]C. E. Shannon and C. Weaver, *The Mathematical Theory of Communication* (University of Illinois Press, Illinois, 1962).
[22]H. Tananbaum, H. Gursky, E. M. Kellogg, R. Levinson, E. Schreier, and R. Giacconi, Astrophys. J. Lett. **174**, L143 (1972).
[23]J. G. Caputo, B. Malraison, and P. Atten, in *Dimensions and Entropies in Chaotic Systems,* edited by G. Mayer-Kress (Berlin, Springer, 1986).
[24]N. B. Abraham, A. M. Albano, B. Das, G. de Guzman, S. Yong, R. S. Gioggia, G. P. Puccioni, and J. R. Tredicce, Phys. Lett. **114A**, 217 (1986).
[25]A. M. Fraser and H. L. Swinney, Phys. Rev. A **33**, 1134 (1986).
[26]A. Ben Mizrachi, I. Procaccia, and P. Grassberger, Phys. Rev. A **29**, 975 (1984).
[27]A. Brandstater and H. L. Swinney, Phys. Rev. A **35**, 2207 (1987).
[28]M. H. Jensen, L. P. Kadanoff, A. Libchaber, I. Procaccia, and J. Stavans, Phys. Rev. Lett. **55**, 2798 (1985).
[29]J. A. Glazier, M. H. Jensen, A. Libchaber, and J. Stavans, Phys. Rev. A **34**, 1621 (1986).